

Ductile cast iron inserts for spent nuclear fuel disposal: digital radiography

F. Lofaj^{1,2*}, L. Metten¹, A. van de Sande¹, K.-F. Nilsson¹, A. Eriksson¹

¹Joint Research Centre – EC, Institute for Energy, P.O. Box 2, 1755 ZG Petten, The Netherlands

²Institute of Materials Research of the Slovak Academy of Sciences, Watsonova 47, 043 53 Košice, Slovak Republic

Received 2 June 2006, received in revised form 15 November 2006, accepted 1 December 2006

Abstract

The acceptance criteria for the canisters for geological disposal of spent nuclear fuel require non-destructive examination (NDE) to check the presence of technological defects. This work is devoted to the investigation of the ability of digital radiography compared to conventional film radiography, to detect defects in ductile cast iron (DCI) insert walls in the Swedish canister concept KBS-3. The advantages of digital radiography include at least three times shorter total examination times, significantly wider dynamic range of the optical densities and possibility for automatic detection of the defects larger than 4 mm. Although its resolution is lower than that of film radiography, it is sufficient with large margin for the detection of the defects in DCI inserts. The total time for the insert inspection using digital radiography with some additional measures can be reduced to 24 h. However, faster automated inspection method, e.g. radioscopy, is desirable for large-scale insert inspection.

Key words: spent nuclear fuel, geological disposal, ductile cast iron, film radiography, digital radiography

1. Introduction

Despite long-term research and experience with numerous nuclear power plants, radioactive waste management is still of concern [1]. Multi-barrier geological repositories of radiotoxic nuclear waste are seen as the most realistic approach providing long-term, cost-effective and safe nuclear waste and spent nuclear fuel disposal [2]. The primary engineered barrier is in this case the canister confining the spent nuclear fuel. A critical issue for the acceptance of the canister is to guarantee that it does not contain defects that may cause loss of integrity during transport and disposal. Non-destructive examination (NDE) of the inserts is necessary to eliminate canisters with potentially dangerous manufacturing defects.

In the first part of this work [3], the capabilities and limitations of the conventional film radiography in detection of defects in ductile cast iron (DCI) inserts used in the KBS-3 canisters were discussed. Radiography was combined with standard microstructure investigation to identify and characterize the indications revealed by radiography. Despite certain prin-

cipal limitations, radiography was found to be suitable for the inspection of the insert walls from the viewpoint of its resolution [3, 4]. High resolution film Agfa Structurix D2 revealed cracks, which are 100 μm wide, more than 1.25 mm deep and volumetric indications larger than 0.4 mm. Medium resolution Agfa Structurix D4 film revealed 100 μm cracks with the depth ≥ 2.5 mm and volumetric defects with the size ≥ 0.67 mm. Maximum detectability of the low resolution film Agfa Curix blue HC-S Plus was ≥ 5 mm for 100 μm cracks and ≥ 0.8 mm for volumetric defects. However, the time necessary for full inspection of the insert walls along the each of 8 fuel channels exceeds several days [3, 4]. This prevents using the film radiography technique for large-scale industrial applications. Obviously, considerably faster techniques, such as digital radiography or radioscopy, have to be explored for this application. In digital radiography, film is replaced by imaging plates, which are scanned for immediate data treatment. However, the resolution of imaging plates is usually lower than for high quality radiographic films. It has to be tested to assure that imaging plates meet criteria for the required defect

*Corresponding author: ¹tel.: +31 22 456 5308; fax: +31 22 456 5641; e-mail address: frantisek.lofaj@jrc.nl

²tel.: +421 557922464; fax: +421 557922408; e-mail address: flofaj@imr.saske.sk

detection. The aim of the current work is to demonstrate the potential of digital radiography compared to conventional film radiography in the detection of the defects in ductile cast iron inserts and its suitability for meeting the acceptance criteria for DCI inserts in the canisters for nuclear waste disposal.

2. Experimental procedure

2.1. Material and sample selection

The parameters of digital radiography system were tested on three different types of samples. They included: i) standard steel reference blocks (RB) with artificial defects; ii) as-produced DCI insert walls with artificial defects and iii) segments from the canister mock-up after stress test, which contained cracks in the insert walls. Both types of DCI segments were taken from I26 insert, which consists of ductile cast iron grade EN-GJS-400-15U (European standard EN 1563) [5]. The studied material was described in details earlier [3]. Thus, the tested samples covered standard procedure for the determination of the system performance as well as testing of the real components with artificial and natural defects.

Image quality indicator blocks. Two different image quality indicator (IQI) standard steel reference blocks with artificial defects were used to determine radiographic sensitivity and flaw detectability of the current radiographic system. The same reference blocks were used also for the evaluation of film radiography [3]. The size of both blocks was 80 mm × 120 mm and their thickness was adjusted to 85 mm. The first reference block (RB 1) called also “IQI crack block” contained four sets of six 100 μm wide grooves with the depths of 15 mm (groove No. 1), 10 mm (groove No. 2), 5 mm (No. 3), 2.5 mm (No. 4), 1.25 mm (No. 5) and 0.6 mm (No. 6). The second reference block (RB 2), called also “IQI groove and hole block” contained a set of thirteen pairs of grooves and holes. The groove widths and hole diameters were equal to their depth and they were 1.6 mm, 1.28 mm, 1.045 mm, 0.83 mm, 0.665 mm, 0.50 mm, 0.42 mm, 0.365 mm, 0.285 mm, 0.22 mm, 0.20 mm, 0.125 mm, and 0.12 mm. The grooves and holes represented volumetric defects with different dimensions and geometry.

Insert walls with artificial defects. Two 200 mm thick segments cut from as-produced I26 insert were used to produce samples with artificial defects. The first segment, referred to as test block 1 (TB1), was a full size cross-section of the insert in the as-produced state (see Fig. 2 in [3]). It contained 8 outer walls with variable wall thickness. Four of them were chosen for testing. A group of three holes with the same diameter was drilled 30 mm deep in axial direction in each of these four insert walls. Figure 1a shows one

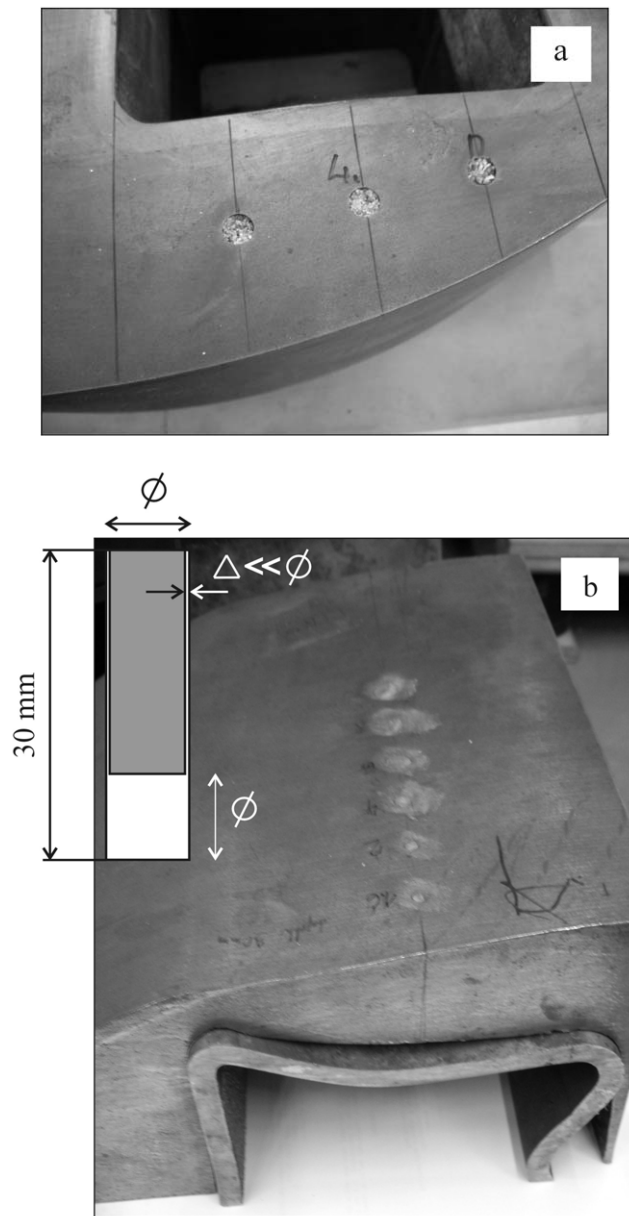


Fig. 1. a) Artificial defects – holes with 10 mm diameter in axial direction – in one of the walls of the 200 mm thick insert slice TB1; b) volumetric defects in test block TB2 with equal wall thickness but variable hole diameter.

set of such holes. The diameters of the holes were 2 mm in the first wall, 3 mm, 5 mm and 10 mm in subsequent walls, respectively. The wall thickness varied from 61.2 mm in the thinnest part to 81.6 mm in the thickest part of the wall. The holes were located along the middle line where the wall thicknesses were approximately 65 mm, 72 mm and 79 mm (the influence of the variation in local wall thicknesses due to the off-sets of the steel tubes was not considered). Thus, the ratio hole diameter/wall thickness between these four hole sets was controlled only by a hole diameter.

Keeping this ratio constant was principally not possible because of much larger range of hole diameter changes compared to wall thickness changes. For 10 mm holes it varied from 0.163 up to 0.122, whereas for 2 mm holes this ratio was in the range from 0.029 to 0.022. The comparison of the visibility between the holes with different diameter has therefore a certain bias.

The empty holes in the walls correspond to the empty blowholes or porosity. However, the critical defects in the studied DCI were considered to be the slag inclusions and oxide filled cracks. To imitate such slag defects artificially, the holes were filled with sand. Sand-filled holes were examined again to reveal the difference compared to the empty holes.

The second sample with the artificial defects (TB2) was only a one-channel segment, which was cut from another full cross-section of the same canister (Fig. 1b). The purpose was to examine isolated volumetric defects deep in the material and simultaneously to reduce the effect of variable defect size/wall thickness ratio. Therefore, six holes were drilled in near-radial direction along the line with the constant wall thickness of 72 mm. The holes were 30 mm deep with diameters 10 mm, 8 mm, 6 mm, 4 mm, 2 mm and 1.6 mm. The closed volumetric defects were imitated in such a way, that each of the holes was partially filled with steel rod of the corresponding diameter. The rods were one diameter shorter than the hole depths. Thus, a set of six closed cylindrical voids at the depth of ~ 30 mm was obtained for digital radiography.

Canister mock-up segments with natural flaws. The natural defects occurring in DCI inserts were examined on the samples cut from the deformed canister mock-up and used earlier for film radiography as described earlier [3, 4, 6, 7]. They contained variety of technological defects [3, 4, 8, 9] and additional cracks formed during hydrostatic loading of this mock-up [6, 7]. The studied sample included a 50 mm slice of an insert segment (see Fig. 3 in [3]) similar to that shown in Fig. 1b. Parts cut of this slice were investigated in axial and radial directions. The results were compared with the images obtained earlier from film radiography [3, 4].

2.2. Digital radiography

Digital radiography was performed using the same sources for the film radiography described earlier [3, 4]. X-ray sources included PHILIPS MCN 451 covering the range of energies up to 450 kV and Varian Linear Accelerator M3 with energies of 1 MeV and 3 MeV. The distances between the source and the film in the setup were 0.9 m and 1.5 m, respectively. The film was replaced by the GE/Agfa IPX imaging plates (20×25 cm² and 15×25 cm² for the channels), which were positioned in a plastic envelope with 0.25 mm



Fig. 2. The system for digital radiography consists of a scanner AGFA RadView CR100 for digitization of the imaging plates, computer with dedicated software and high-resolution monitor.

lead intensifier screen and 5 mm lead back plate. The images were digitized using dedicated scanner (model RADView CR 100, Agfa/GE Inspection Technologies, USA) with the pixel size of 100 μm (Fig. 2).

The conditions for the optimum exposure were determined for each sample and source. Compared to the conventional film, a slightly lower accelerating voltage, a 50 % lower current and shorter exposure time provided the optimum optical density. The images were digitally manipulated after digitization using dedicated software (RADView Workstation Ver. 3.9) and high resolution monitor.

3. Results

3.1. Digital radiography

The optimum exposure condition for imaging plates in the outer channel walls of the insert was 400 kV at 4 mA current for 1 min. The tests on the reference block RB1 revealed that grooves No. 1 through No. 4 (2.5 mm depth) could be visualized on the IPX plates. In the RB2 block, the 0.83 mm hole and groove and parts of a 0.665 mm hole and groove could be detected as the smallest indication.

Figure 3 shows side view of TB1 insert wall from Fig. 1a with three 10 mm holes at the top. Despite variable wall thickness, the whole width of the wall is within the reasonable range of optical densities. Thus, it is possible to examine the entire wall in one shot. All three empty holes are also visible at the top in Fig. 3. The same measurements were repeated with the holes filled with sand. The optical density expressed in terms of grey level (note the difference from optical density, D , used in film radiography which is determined from the ratio of intensities of the light

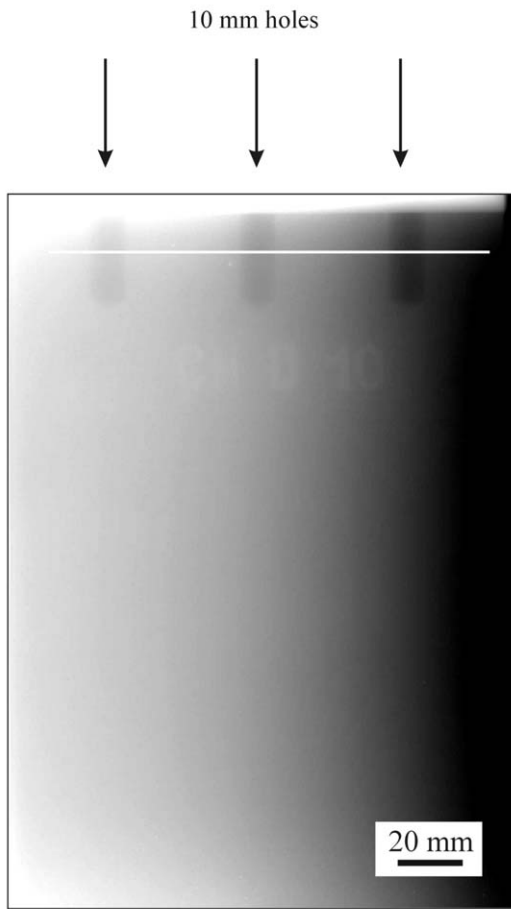


Fig. 3. Radiographic images of the insert wall with three 10 mm diameter holes obtained from the imaging plates. The optical density of the image was measured along the indicated line.

incident and transmitted through the film) was measured on both images along the horizontal line passing through these holes (see Fig. 3). Its distributions along the corresponding lines from empty and filled holes are compared in Fig. 4. Both curves follow the same tendency – intensity increases non-linearly as wall thickness decreases. The intensity peaks correspond to the holes. The main parameter obtained from these curves is the change in optical density at the holes, Δd . It was determined as a difference between the base background curve and the peak value for the corresponding hole (see Fig. 4). The same procedure was repeated for each set of holes. Though they were visible by eye, the differences in the measured intensities in the case of 3 mm and 2 mm holes were very close to the background noise variations. Therefore, they were not considered. The values of Δd are plotted as function of hole diameter in Fig. 5. Open squares in this plot refer to the empty holes, full squares – to the holes with sand. The differences in terms of Δd for the holes with the same diameter result from the change in hole diameter/wall

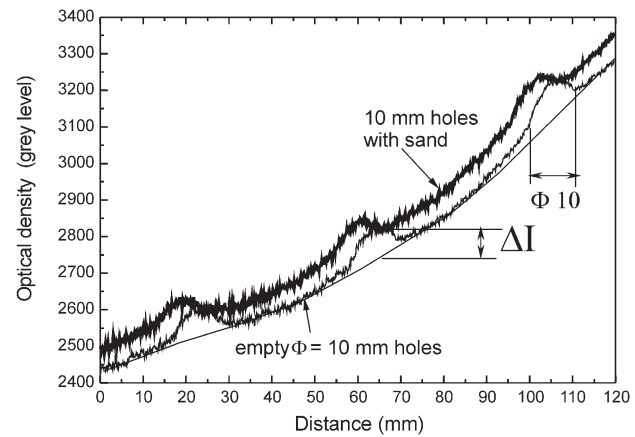


Fig. 4. Profiles of the digital “optical” density across the holes with the diameter of 10 mm.

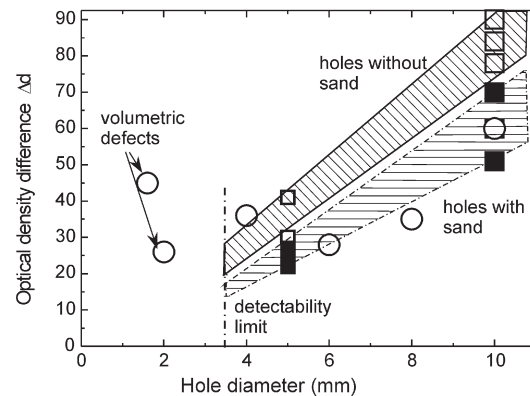


Fig. 5. “Optical” density differences in the holes with different diameter for empty holes, holes filled with sand, which model slag inclusions and volumetric defects as function of hole diameter. The differences for 3 mm and 2 mm holes were below the resolution limit.

thickness ratio. The greatest Δd were always obtained for greater ratio, i.e. for thinner part of the wall. Despite that, the behavior within the measured defect size range and range of (hole diameter/wall thickness) ratios roughly follows linear dependence. The same is valid also for sand-filled holes but the range of the slopes is slightly smaller.

The same measurements were repeated for the TB2 sample with artificial volumetric defects (Fig. 1b). Optical density was measured along the line passing through the centers of the voids. The profile of the optical densities is illustrated in Fig. 6. Obviously, another background profile compared to that in Fig. 4 and additional peaks present at the defect edges have to be explained. Despite constant wall thickness in this case, the effective wall thickness for an X-ray beam from a point source corresponds to the true wall thickness only in normal direction and increases proportionally to the angle measured from the normal direc-

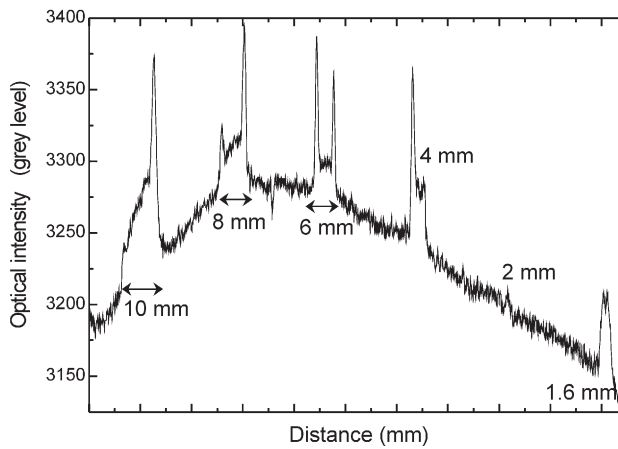


Fig. 6. Profile of the grey level “optical” density across the artificial volumetric defects with different size and constant wall thickness.

tion. The background intensity reaches maximum at the normal to the beam source and decreases in other directions. Such dependence can be eliminated using baseline intensity fitting the background intensity profile.

The edge effects result from the way the volumetric defects were made. The fits between the hole diameters and filling rods were not tight and narrow gaps existed along the perimeter of the rods (see Fig. 1b). The length of these gaps was around 30 mm and it was projected on the imaging plate. This caused an increase of the optical intensity of the X-ray beam at the perimeter of the holes similarly as in the case of cracks with the same size and orientation. True Δd was considered to correspond to the intensity between the background line and the lowest or mean value between the edge peaks on each hole. Note the difficulties with 1.6 mm and 2 mm defects. Their edge effects overlap and the values of Δd , indicated in Fig. 5 by open circles, are out of reasonable range. Therefore, the values obtained for these two defects were excluded from further analysis. The Δd values for the remaining defects are slightly lower than the data from empty holes and fall in the zone of sand-filled holes. However, the agreement between both sets of experimental data is acceptable.

Reliable and faster detection of the defects is the most important expectation from digital radiography. Figures 7a and 7b illustrate wide dynamic range of IPX plates in the case of the inspection of the insert wall of the I26 mock-up sample in radial direction. The contrast and brightness were adjusted digitally in such a way that both thinner (Fig. 7a) and thicker part of the wall (Fig. 7b) can be inspected. Figure 7c shows this wall using D4 film. Rather weak but the same indication – an agglomerate of slag inclusions – can be seen in both cases. The main difference between

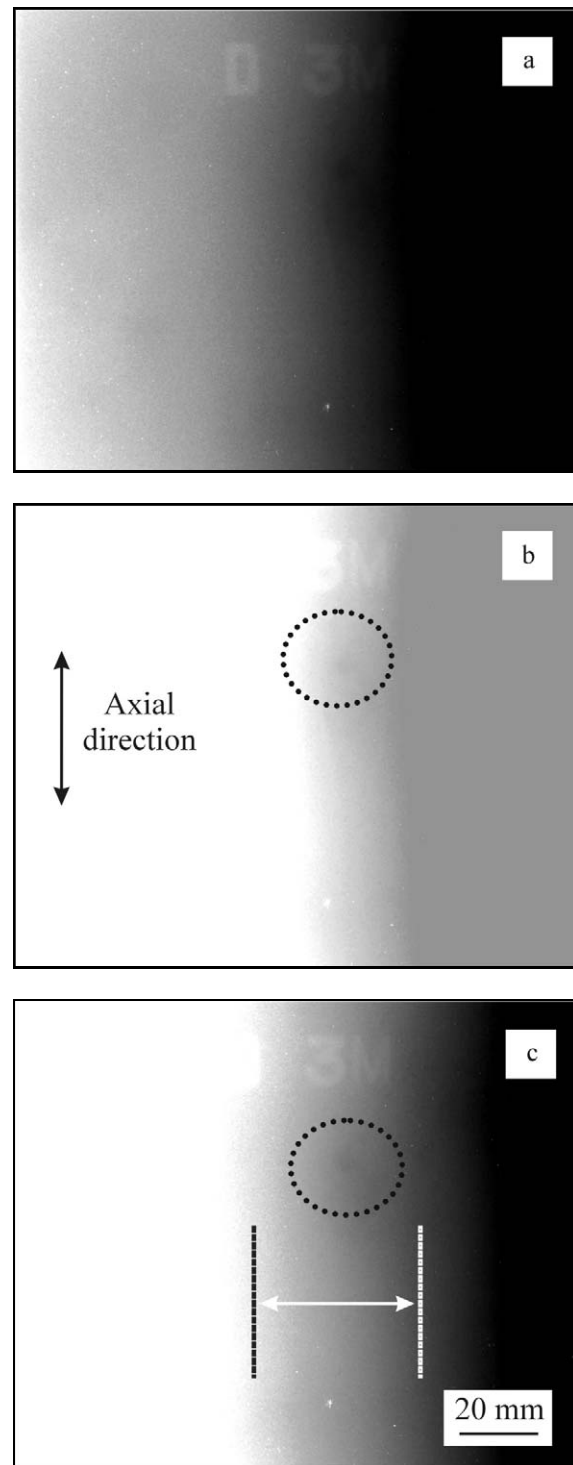


Fig. 7. Wide dynamic range of digital plates enables manipulation of the image contrast and brightness to inspect both thinner (a), and thicker (b), zones of mock-up walls on one image. Only relatively narrow zone can be examined when using conventional films (c). Weak indication of the inclusion is indicated for both cases.

both images is in the width of the zone, which can be examined. Digital plates enable inspection across the

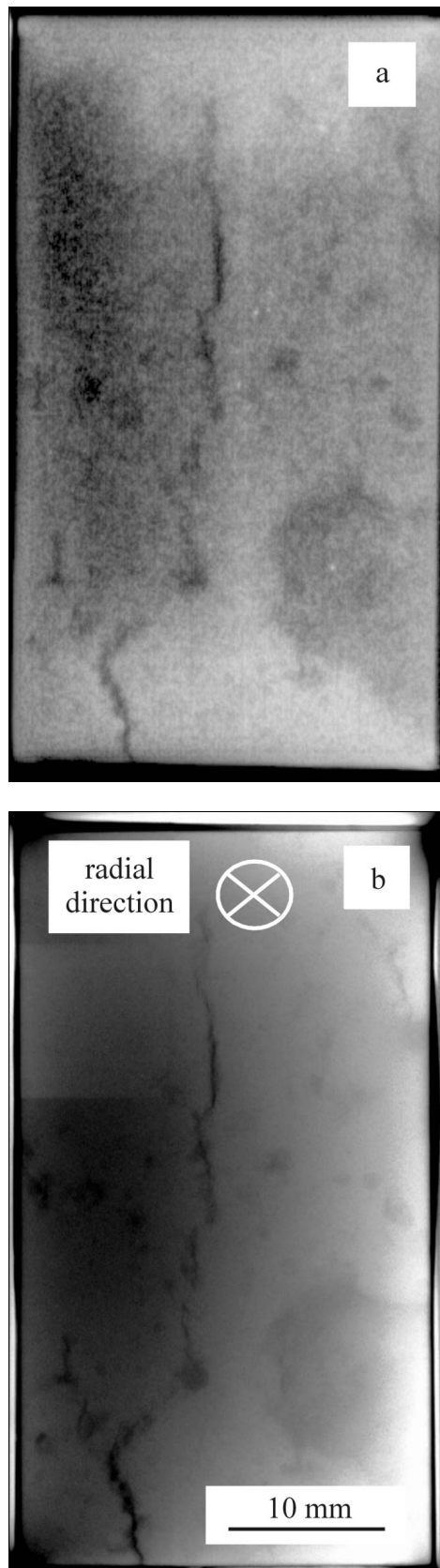


Fig. 8. The comparison of the radiographic images of the cracks in the mock-up wall in radial direction obtained from a) IPX imaging plate and b) conventional D2 film.

whole insert wall whereas the range of the suitable optical densities on conventional films is only around 1/3 of the wall thickness during one exposure.

Figure 8 is a comparison of the magnified images of the large cracks formed during the pressure test in the mock-up wall. The images are almost identical but more details can be seen on the image from the film radiography. The effect of dynamic range is less important in this case because of small wall thickness variation in this case.

The examination of the cracks in the direction perpendicular to their fracture surface by digital radiography showed the same results as conventional radiography – cracks are not detectable and only slag inclusions were visible in this case.

4. Discussion

4.1. Resolution of digital vs. film radiography

The optimum exposure condition for the outer channel walls in the case of imaging plates was 400 kV accelerating voltage and 4 mA current for 1 min compared to 450 kV, 10 mA and 2 min exposure time in D2 film. Thus, digital radiography requires less time and lower accelerating voltage and smaller current than conventional film. The range of the optimum optical densities is 1.1, which is only slightly larger than 1.0 for D2 film. However, the dynamic range of IPX plates is much larger than for conventional films. Because of that, the whole width of the insert wall can be examined after one exposure, whereas at least three exposures are necessary when using D2 film or two exposures with D4 film. The resolution is, however, lower for the digital radiography.

The tests with the reference block RB1 revealed that 100 μm wide grooves with depth of at least 2.5 mm can be detected using IPX plate. This corresponds to the resolution D4 film and half of the resolution of D2 film. The same is valid in the case of volumetric defects. IPX plate can reliably resolve 0.8 mm hole, which is the same as D4 film, whereas D2 film resolves 0.4 mm holes. Thus, digital radiography using IPX plates provides around half of the resolution of the D2 film and it is equal to medium resolution D4 film. These results are valid for the steel reference blocks. The resolution limits in the case of real ductile cast iron components with more complex geometry and larger thickness can be determined from the data in Fig. 5. This plot shows approximately linear (within the studied range) increase of Δd with the increase of the defect size. The value of Δd corresponds to the difference in optical densities resulting from the change of beam intensities when passing through the material with the defect and without the

defect. The defects, e.g., an empty blownhole, would effectively reduce the thickness of the sample, which increases an intensity of the beam at the recording film or plate. Filling the blownhole with the sand reduces this difference because the beam is losing additional energy when passing through sand. Thus, lower slope was obtained for the sand-filled holes in Fig. 4. The same argument is valid for the understanding of the defect size/wall thickness ratio. The defects with larger relative size absorb less beam energy than those with smaller relative sizes. Therefore, Δd is larger in thinner part of the insert wall and *vice versa*.

Figure 5 allows us to estimate the lower detection limit. Although even 2 mm defects were visible on RB1 and RB2 by human eyes, they were not reliably detectable in the plot because the scatter in measurement was comparable to scatter of the background signal. The Δd values, which are sufficiently large to be reliably determined from Fig. 4 or extracted automatically from simple image analysis, can be obtained for the defects at about 4 mm in size. Thus, as indicated in Fig. 5, the limit size for the studied defect detection is around 4 mm.

Figures 7 and 8 confirmed the ability of digital radiography to visualize most of the inclusions and cracks detectable by conventional radiography despite lower resolution. Although the image quality from digital plate is lower compared to the D2 film, it can be concluded that digital radiography is a reliable tool for the detection of medium to large cracks in cast iron canisters.

4.2. Suitability of digital radiography for insert inspection

At least two additional questions have to be discussed prior to the conclusion on the suitability of digital radiography for the insert inspection. The first question is whether the obtained resolution of digital radiography of 4 mm is sufficient. The answer requires a comparison with the critical size defects. They were calculated by Dillström [10] for the local tensile stresses from finite element analysis [11] of the insert walls when the canister is subjected to external hydrostatic pressure. The results in Fig. 9 show that the critical defect size depends on the external stress and geometrical factors, especially on the off-set of the steel tubes. The off-set, δ , is defined as a deviation from the ideal cylindrical symmetry with regard to outer insert wall, which causes reduction (or increase) in the thickness of the outer walls of the canister. It was found that for the offsets less than 5 mm, critical defect size is larger than 30 mm stresses up to 50 MPa. In the case of 10 mm off-set, critical defect size decreased from 30 mm at 45 MPa to 10 mm at 48 MPa and to 2 mm at 50 MPa. Obviously, reduction of δ to less than 5 mm is the most effective way to reduce stress

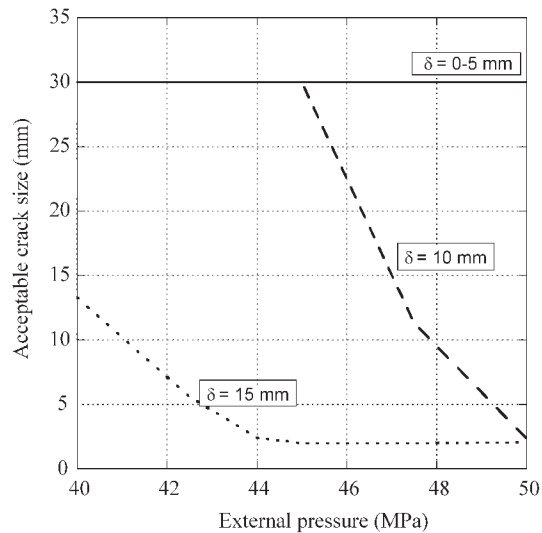


Fig. 9. The critical defect size in the DCI walls in the range of external hydrostatic stresses from 40 MPa to 50 MPa and for the off-sets of the steel tubes from 0 mm up to 15 mm from the ideal cylindrical symmetry [10].

concentration and failure probability of the insert. In the case of $\delta < 10$ mm, critical defect size of 30 mm is much larger than slag agglomerates and oxide-filled cracks (max. 5 mm) reported earlier [3, 4, 8, 9]. Even the largest blownholes, which were observed only in the inner walls of the inserts zone [4], were considerably smaller than the critical defects. The comparison of critical defect sizes at small and moderate off-sets with the size of defects, which are detectable by digital radiography, results in the margin to detection of around 7. Thus, the resolution of digital radiography exhibits sufficiently high margin for the inspection of insert walls.

The main practical problem with film radiography for insert examination is the excessive time required for full insert inspection (> 6 days). The expected production rate is 1 canister per day, which determines also the maximum time for the inspection. The minimum time necessary for the inspection of 20 cm long insert wall by the used digital radiography system is from 12 to 15 minutes. It includes loading the plate into the channel (1 min), exposure and discharging (2–3 min), extraction of the image plate, its loading into scanner, scanning and erasure (5 min), manipulation of the image and search for the defects (4–6 minutes). The image after scanning is totally gray and the defect data have to be extracted using contrast enhancement. However, due to wide dynamic range of digital imaging plates, the optimum contrast and brightness can be adjusted and defects gradually visualized across the whole wall width. Conventional radiography would require for the same task at least 3 exposures.

Assuming that 20 cm long imaging plate is used,

the inspection of all 8 insert walls with the length of 5 m each would require 200 exposures. This corresponds to around 50 hours for the examination. Thus, although digital radiography leads to significant reduction of the examination time compared to film radiography, it is still more than twice of the acceptable time. Inspection time can be possibly shortened using slightly longer and faster imaging plates, automated systems for plate loading, retrieval from the insert channels and analysis of the images based on the optical density contrast or to the inspection of only upper part of the insert, where slag defects concentrate. When all these measures are applied, the total inspection time can be reduced to approximately 24 hours, which is already close to the upper acceptable limit. However, even faster non-destructive examination techniques, e.g. automated radioscopy, are desirable for large-scale insert production.

The investigation of the suitability of ultrasonic methods for non-destructive examination of the inserts is also a part of the current project [3]. Principal advantages of ultrasonic techniques compared to radiography include easier handling because there is no irradiation. Another advantage is that it can be much faster. However, the analysis of the data and defect detection are very difficult on components with variable wall thickness and relatively complex geometry. Both radiography and ultrasonic methods are complementary and may be combined to assure the acceptance criteria.

5. Conclusions

The comparison of digital (IPX plates) vs. conventional film radiography applied to the inspection of DCI inserts for the canisters for nuclear fuel disposal suggests the following conclusions:

- The advantage of the IPX imaging plate is wider dynamic range, which is suitable for objects with large thickness variations. Moreover, the system does not need a chemical development process, imaging plate are reusable and the whole examination cycle is 2–3 times faster than conventional film radiography.

- The time for full digital radiography examination of the insert walls is expected to be at least three times shorter than with conventional radiography and can be reduced to 24 h when additional measures are used. However, even faster automated inspection method, e.g. radioscopy, is desirable for large-scale insert production.

- Appropriately oriented cracks as well as slag inclusions and blowholes with the size exceeding 4 mm can be reliably detected. System can be ultimately used for automatic detection of defects with appropriate size and orientation.

- Although the resolution of IPX plates is lower than in the current high-resolution radiographic films, it is sufficient with large margin for the examination of the defects in DCI inserts.

References

- [1] OJOVAN, M. I.—LEE, W. E.: An Introduction to Nuclear Waste Immobilisation. Oxford, Elsevier 2005.
- [2] Programme for research, development and demonstration of methods for treatment and final disposal of nuclear waste, including social impact research. Swedish Nuclear Waste Management 2004. Available at www.skb.se
- [3] LOFAJ, F.—METTEN, L.—VAN DE SANDE, A.—NILSSON, K.-F.—ERIKSSON, A.: Kovove Mater., 45, 2007, p. 17.
- [4] LOFAJ, F.—METTEN, L.—VAN DE SANDE, A.—SELDIS, T.—NILSSON, K.-F.—ERIKSSON, A.: Ultrasonic and Radiography Investigations of Defects in Ductile Cast Iron Casks for Disposal of Spent Nuclear Fuel. Eureport EUR 22145 EN, DG JRC – Institute for Energy, Petten, The Netherlands 2005.
- [5] NEN-EN 1563:1997, European standard, Founding-Spheroidal graphite, CEN, 1997.
- [6] NILSSON, K.-F.—LOFAJ, F.—BURSTRÖM, M.—ANDERSSON, C.-G.: Pressure tests of two KBS-3 canister mock-ups. Technical report TR-05-18, Svensk Kärnbränslehantering AB, Sweden 2005. Available at www.skb.se
- [7] NILSSON, K.-F.—BURSTRÖM, M.—LOFAJ, F.—ANDERSSON, C.-G.: Eng. Failure Analysis, 14, 2007, p. 47.
- [8] NILSSON, K.-F.—BLAGOEVA, D.—MORETTO, P.: Eng. Fracture Mechanics, 73, 2006, p. 1133.
- [9] NILSSON, K. F.—MINNEBO, P.—BLAGOEVA, D.: J. Mat. Eng. Performance, 2006 (in press).
- [10] DILLSTRÖM, P.: Private communication (presentation KBS-3 Integrity Review meeting, Stockholm, Sweden, January 10, 2006).
- [11] DILLSTRÖM, P.: Probabilistic analysis of canister inserts for spent nuclear fuel. Technical report SKB TR-05-19, Svensk Kärnbränslehantering AB, Sweden 2005. Available at www.skb.se